

Scaffolds for Tympanic Membrane Regeneration in Rats

Yi Shen, MBBS,¹⁻³ Sharon Leanne Redmond, Assoc Dip Appl Sci (Biol),^{1,2} Bing Mei Teh, MBBS,^{1,2} Sheng Yan, PhD, MD,⁴ Yan Wang, PhD,⁴ Lin Zhou, PhD,⁴ Charley A. Budgeon, BSc,⁵ Robert Henry Eikelboom, PhD,^{1,2} Marcus David Atlas, FRACS,^{1,2} Rodney James Dilley, PhD,^{1,2} Minghao Zheng, PhD, MD, FRCPath,^{4,6} and Robert Jeffery Marano, PhD^{1,2}

Tympanic membrane (TM) perforations lead to significant hearing loss and result in possible infection of the middle ear. Myringoplasty is commonly performed to repair chronic perforations. Although various grafts and materials have been used to promote TM regeneration, all have associated limitations. The aim of this study was to evaluate the efficacy and feasibility of two graft materials, silk fibroin scaffold (SFS) and porcine-derived acellular collagen type I/III scaffold (ACS), compared with two commonly used graft materials (paper patch and Gelfoam) for the promotion of TM regeneration. These scaffolds were implanted using on-lay myringoplasty in an acute TM perforation rat model. Surface morphology of the scaffolds was observed with scanning electron microscopy. The morphology of the TM was assessed at various time points postimplantation using otoscopy, light and electron microscopy, and functional outcomes by auditory brainstem responses. We found that SFS and ACS significantly accelerated the TM perforation closure, obtained optimal TM thickness, and resulted in better trilaminar morphology with well-organized collagen fibers and early restoration of hearing. However, paper patch and Gelfoam lost their scaffold function in the early stages and showed an inflammatory response, which may have contributed to delayed healing. This study indicates that compared with paper patch and Gelfoam, SFS and ACS are more effective in promoting an early TM regeneration and an improved hearing, suggesting that these scaffolds may be potential substitutes for clinical use.

Introduction

TYMPANIC MEMBRANE (TM) perforation is one of the most common problems in otolaryngology. If left untreated, it is associated with significant morbidity such as hearing loss, recurrent otorrhea, middle ear infection, and acquired cholesteatoma.¹ Although most acute TM perforations heal spontaneously, large or chronic TM perforations, especially from chronic suppurative otitis media, often fail to heal and may require grafting.²

Currently, surgical methods such as myringoplasty are regarded as the most effective and reliable treatment for TM perforations.^{3,4} Various autologous grafts and allografts such as muscle fascia, cartilage, perichondrium, and AlloDerm have been used; however, all have their own limitations.⁵ For instance, temporalis fascia, which is regarded as the “gold standard,” is associated with donor site morbidity,

additional incisions, long operation time, and a shortage of material in revision cases.⁵ AlloDerm, derived from human cadaver donor skin, is almost 10 times thicker than the normal TM, and its use is limited by the shortage of suitable human donors.⁶ To date, a range of xenografts and synthetic materials, including Gelfoam,⁷ paper patch,⁸ and hyaluronic acid derivatives,⁹ have been investigated as suitable scaffolds that support the regeneration of TM. However, little evidence supports any of these as optimal materials for various types of perforations.¹⁰ Moreover, several commercially available xenografts such as porcine small intestinal submucosa may evoke an inflammatory response due to the remnant xenocellular components, including serotonin.^{11,12} In addition, many synthetic materials are nonbiodegradable, and their biomechanical and material properties are different compared with the normal TM, which may affect the long-term hearing function.⁵ Hence, there is a constant

¹Ear Sciences Centre, School of Surgery, The University of Western Australia, Nedlands, Australia.

²Ear Science Institute Australia, Subiaco, Australia.

³Departments of Otolaryngology and Head & Neck, Ningbo Medical Centre, Ningbo Lihuili Hospital, Ningbo, China.

⁴Key Laboratory of Combined Multi-organ Transplantation, Ministry of Public Health; Division of Hepatobiliary and Pancreatic Surgery, Department of Surgery; The First Affiliated Hospital, School of Medicine, Zhejiang University, Hangzhou, China.

⁵Centre for Applied Statistics, The University of Western Australia, Perth, Australia.

⁶Centre for Orthopaedics Research, School of Surgery, The University of Western Australia, Nedlands, Australia.

search for better materials to achieve improved healing and hearing.

Recently, with the advances in materials for tissue engineering, various alternative biomaterials have been developed as artificial eardrums for TM repair; these include silk,¹³ collagen,^{14,15} chitosan,¹⁶ and calcium alginate.¹⁷ Silk fibroin, a protein polymer obtained from silkworm silk, possesses ideal properties such as biocompatibility, biodegradability, high tensile strength, and elasticity.^{18,19} More importantly, human TM keratinocytes have been shown to adhere and proliferate successfully on silk fibroin membranes *in vitro*.^{20,21} Collagen, a major extracellular matrix component, also has desirable physical characteristics such as high tensile strength, flexibility, nonreactivity, nontoxicity, and noncarcinogenicity.^{7,22} As the main constituent of the lamina propria of the TM, collagen helps in maintaining the resilience and integrity of the TM and, hence, plays a key role in hearing.^{23,24} However, only limited studies on silk and collagen as TM scaffolds have been performed, and the hearing outcomes for these scaffold materials have yet to be investigated. Hence, the aim of this study was to evaluate the efficacy (healing and hearing outcomes) of silk fibroin scaffold (SFS) and porcine-derived acellular collagen type I/III scaffold (ACS) as scaffolds for TM regeneration compared with more commonly used materials such as paper patch and Gelfoam in an acute TM perforation rat model.

Materials and Methods

Description of scaffolds

Silk fibroin scaffold. SFS was prepared by the Institute for Frontier Materials, Deakin University, Geelong, Australia, as previously described by Rajkhowa *et al.*²⁵ This formic acid-based silk film is ~30 μm thick, transparent, and has high tensile strength.

Acellular collagen type I/III scaffold. ACS was manufactured and supplied by Orthocell Ltd. This collagen scaffold is derived from porcine peritoneum, decellularized, and processed to a thickness of ~40 μm . The manufacturing process can be referred to the patent titled "Method for manufacture collagen scaffold" (Cellgro™; Patent No 2008901451/PTO).

Paper patch. Paper patch was obtained from cigarette paper (Tally Ho; Imperial Tobacco Australia). It is ~20 μm thick, white, and opaque.

Gelfoam®. Gelfoam (absorbable gelatine sponge, Pharmacia & Upjohn, Inc.) is a highly absorbent, nonelastic sponge that is around 4 mm thick with its pore size varying between 30 and 700 μm .²⁶ Gelfoam was supplied sterile in its original packaging, while the other three materials were sterilized with ethylene oxide gas.

Animal models

The experimental protocols were approved by both the Animal Ethics Committees at The University of Western Australia (Australia) and Zhejiang University (China). One hundred and sixty male Sprague–Dawley rats, weighing

250–300 g, were obtained from Shanghai Animal Center (Chinese Academy of Science, Shanghai, China). All rats were housed in the experimental animal facility of the Zhejiang University and were provided with food and water *ad libitum* in a room with 12-h light/dark cycles. Before the study, all animals were inspected using a S5 model otomicroscope (Zeiss) to ensure they were free of middle ear pathology. A total of 150 rats were randomly divided into four scaffold repair groups, namely SFS ($n=30$), ACS ($n=30$), paper patch ($n=30$), Gelfoam ($n=30$), and control (spontaneous healing) ($n=30$). In addition, a group of 10 rats ($n=10$) were allocated as normal controls (without any perforation or scaffold).

All the surgical procedures were performed under general anesthesia with intramuscular Ketamine (80 mg/kg) and Medetomidine (0.5 mg/kg). Debris from the external auditory canal was removed using a 3.0 mm aural speculum, and the external auditory canals were prepped with povidone iodine solution. Bilateral TM perforations, measuring ~1.8 mm in diameter, were created using a sterile 23-gauge needle in the posterior half of the pars tensa via a transcanal approach. Four different materials were then trimmed into pieces (2.4 mm in diameter), rinsed with 1 \times phosphate-buffered saline solution (pH 7.4) (Invitrogen), and grafted onto the right TM perforation using on-lay myringoplasty. Ofloxacin ointment (Tarivid® eye ointment; Santen Pharmaceutical Co., Ltd.) was applied to the margin of the scaffolds to maintain the scaffolds in place. For ACS, the rough surface was placed medially so that the smooth surface faced toward the external auditory canal. The left ear served as an internal control where no graft material was placed on the perforated TM. All rats were given subcutaneous buprenorphine (0.02–0.08 mg/kg) for postoperative analgesia.

Healing of the right ear TM in different treatment groups was evaluated by otoscopy, scanning electron microscopy (SEM), histology, and transmission electron microscopy (TEM); while the hearing function was analyzed by auditory brainstem responses (ABR). Left ears were not evaluated. In each group, five rats ($n=5$) were selected randomly for both otoscopic and ABR assessment at 3, 5, 7, 9, 14, and 28 days postoperatively. In these subgroups of five rats, three were used for histological evaluation, and one each was used for SEM and TEM.

Otosopic observation

To investigate TM healing, five rats from each group were randomly chosen at each time point for otoscopic observation using a digital video otoscope (MedRX) under general anesthesia. The TMs were viewed by two independent observers with regard to perforation closure, infection, myringosclerosis, granulation tissue, and thickening. Each TM perforation was graded as either completely closed or unclosed. Only TMs that had completely closed were considered healed. Digital images were recorded using Aurisview software (Ear Science Institute Australia, Subiaco, Australia).

Scanning electron microscopy

SEM was performed to characterize the surface morphology of four individual scaffolds. Briefly, the scaffold samples

were sputter coated with 5 nm thick platinum (SEM coating unit, E 1020; Hitachi Science Systems Ltd.), and both sides were viewed under a scanning electron microscope (S260; Leica) at a low voltage (20 kV).

In addition, SEM was performed to evaluate the healing process of TM after repair by scaffolds. Briefly, the rat TM specimens were fixed with 2.5% glutaraldehyde in 4°C overnight, dehydrated in ethanol solutions followed by critical point drying (HCP-2; Hitachi). Finally, the samples were coated with 5 nm thick platinum, where the medial surface of the TMs was observed under SEM.

Histological evaluation

After sacrifice, right external ears were separated at the osteocartilaginous junctions, and the TMs along with the bony annulus were removed from the tympanic bulla. Harvested specimens were fixed in 10% neutral buffered formalin for 24 h followed by decalcification in 10% ethylenediaminetetraacetic acid solution (pH 7.4) for 2–3 weeks. Decalcified TMs were dehydrated in a series of graded alcohols, embedded in paraffin wax, and transversely sectioned at a thickness of 4 μm. All sections were evaluated using hematoxylin and eosin staining. Masson's trichrome staining was performed to examine the morphology of collagen fibers. All stained slides were digitally scanned using an Aperio ScanScope XT automated slide scanner (Aperio Technologies, Inc.; 40×/0.75 Plan Apo objective). Images were saved as SVS files for histological evaluation. TM thickness of healed TM sections on days 14 and 28 was measured using Aperio ImageScope Viewer software.

Transmission electron microscopy

TEM was performed to investigate the microstructure of the healed TMs on day 28 postrepair. Briefly, after dissection, the perforation site of the harvested TM samples was fixed in

2.5% glutaraldehyde and stored overnight at 4°C. Tissue specimens were washed, postfixed (1% osmic acid), dehydrated, and embedded for transmission observation. Thin transverse sections were cut and examined with TEM (TECNAI 10, Philips Co.) at 80 kV.

Auditory brainstem responses

To assess the hearing of rats after grafting, ABR was performed using the Nihon Kohden Neuropack-μ Measuring Systems (MEB-9100; Nihon Kohden) in a soundproof room. Rats were anesthetized before testing as previously described. Platinum subdermal needle electrodes were inserted at the scalp vertex (active electrode), both mastoids (reference electrode) and at the nose tip (ground electrode). The test stimuli (click) with 0.1 ms duration were presented through an insert earphone. Animals were presented with a stimulus intensity series from 90- to 0-dB sound pressure level in 10-dB decrements. A total of 512 responses were averaged in each series of stimuli over a 10 ms analysis period. Thresholds were defined as the lowest intensity to elicit a reproducible ABR waveform with typical wave III or wave IV morphology. Auditory thresholds of click stimuli were measured pre- and post TM perforation in the right ear of all rats, and at each time point after myringoplasty for the five animals from each group. The normal ears and the ears with TM perforation without materials served as controls.

Statistical analysis

Healing rates determined by otoscopic observation were compared using the chi-square test. Statistical analysis for ABR and TM thickness was evaluated using one-way analysis of variance, whereas hearing recovery in each group over time was performed using multiple linear regression analysis. All analyses were performed using the Statistical Software R (Version 2.11.1, package meta). Statistical significance was defined as $p < 0.05$.

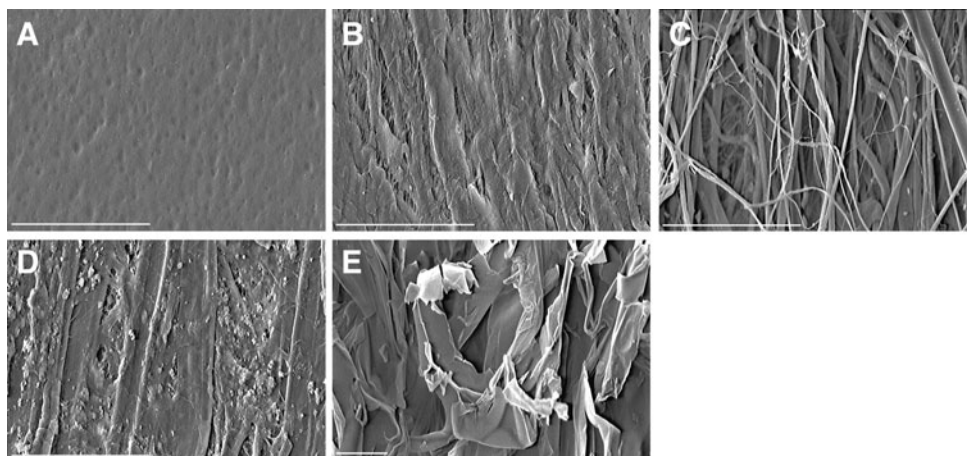


FIG. 1. The surface morphology of scaffolds. Scanning electron microscopy (SEM) showed the surface morphology of four scaffolds (A–D; ×500, E; ×200). Silk fibroin scaffold (SFS) was characterized by a smooth, dimpled, and nonporous surface (A). Acellular collagen type I/III scaffold (ACS) possessed two distinct surfaces: a smooth surface featuring compact collagen bundles (B), and a rough, porous surface of loose collagen fibers (C). Paper patch surface was uneven with a few small pores (D). Gelfoam showed substantial pores of varying sizes (E). Scale bar: 500 μm.

Results

Morphological characterization of scaffolds

SEM of scaffolds before implantation showed that SFS was characterized by a smooth and nonporous surface (Fig. 1A). ACS had two distinct surfaces: a smooth surface with compact collagen bundles (Fig. 1B) and a rough, porous surface with loose collagen fibers (Fig. 1C). Paper patches demonstrated an uneven surface topology with a few small pores (Fig. 1D). In contrast, Gelfoam showed substantial pores of varying sizes (Fig. 1E).

Promotion of TM regeneration induced by scaffolds

Otoscopic observation. An acute rat model of TM perforation was successfully established. All rats survived the surgical procedures with no complications postoperatively. The lateral aspect of TMs was observed via an otoscope to assess the effect of grafting at each time point. No signs of infection or abnormalities were observed in any of the rats.

In the control group, the TMs appeared thicker and opaque postperforation, with prominent microvessels visible

close to the perforation margin. By 14 days, the TM became increasingly transparent, and a majority of the perforations had fully closed. At 28 days, all the perforations were completely healed, although visible scars resembling an opalescent ring were observed at the perforation site (Fig. 2). The transparency of SFS and semi-transparency of ACS allowed direct observation of the TM healing. Throughout the healing process, both SFS and ACS retained their structural stability and adhered well to the TM remnant. The opacification of TM and microvessels was less pronounced compared with those in the control group. The perforations had healed as early as 7 days after grafting where the healed TMs appeared normal (Fig. 2). In contrast, paper patch and Gelfoam were opaque, making it difficult to examine the middle ear during healing. Moreover, these materials tended to detach easily from the healing TM. In particular, the bulk of Gelfoam shrank, and its porous structure was lost over time. At 28 days, the TMs in the paper patch and Gelfoam groups appeared healed but with some scarring (Fig. 2).

After sacrifice at individual time points, closure of the perforation was confirmed by observing the internal surface of the harvested TMs using an otomicroscope. TM healing in

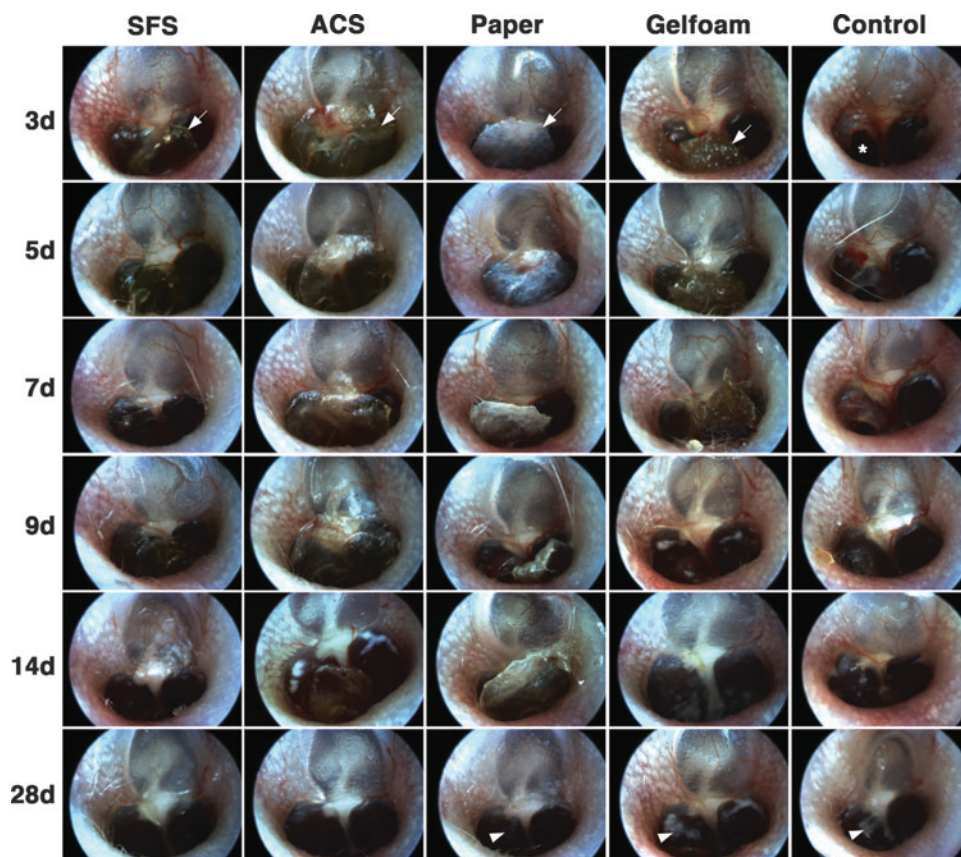


FIG. 2. Otoscopic observation of tympanic membrane (TM) healing after grafting. The lateral aspect of TMs was observed with otoscopy. The transparency of SFS (fully transparent) and ACS (semi-transparent) allowed direct observation of the TM healing, whereas the opacity of paper patch and Gelfoam resulted in difficulty with examination. SFS and ACS adhered well to the TM remnant throughout the healing process; however, paper patch and Gelfoam partially detached at 7 days. Microvessels were most prominent in the control group (3–14 days) compared with scaffold-treated TMs. Perforation closure of SFS and ACS was observed at 7 days compared with 9 days in the paper and Gelfoam groups and 14 days in the control group. Scar formation was visible at 28 days in the paper patch, Gelfoam, and control groups (white arrowheads). White arrows indicate scaffolds; asterisk indicates perforation.

TABLE 1. HEALING OF TYMPANIC MEMBRANE PERFORATION AT DIFFERENT TIME POINTS AFTER GRAFTING

Group	3 days (n=5)	5 days (n=5)	7 days (n=5)	9 days (n=5)	14 days (n=5)	28 days (n=5)
Silk fibroin scaffold	0/5 (0.0%)	1/5 (20.0%)	4/5 (80.0%) ^a	5/5 (100%) ^a	5/5 (100%)	5/5 (100%)
Acellular collagen type I/III scaffold	0/5 (0.0%)	0/5 (0.0%)	3/5 (60.0%) ^a	5/5 (100%) ^a	5/5 (100%)	5/5 (100%)
Paper patch	0/5 (0.0%)	0/5 (0.0%)	2/5 (40.0%)	5/5 (100%) ^a	5/5 (100%)	5/5 (100%)
Gelfoam	0/5 (0.0%)	0/5 (0.0%)	0/5 (0.0%)	3/5 (60.0%)	5/5 (100%)	5/5 (100%)
Control	0/5 (0.0%)	0/5 (0.0%)	0/5 (0.0%)	2/5 (40.0%)	4/5 (80.0%)	5/5 (100%)

^a $p < 0.05$, statistically significant difference between control (spontaneous healing) and the other scaffold.

the SFS and ACS groups was markedly quicker compared with the other groups (Table 1). In fact, one TM in the SFS group had healed as early as day 5. At 7 days, TMs had healed in 80% (4/5) of SFS-treated ears and in 60% (3/5) of ACS-treated ears; while none had healed in the control group (0/5) ($p < 0.05$). After 9 days, the TM was completely healed in all five rats in the SFS, ACS, and paper patch groups, which was significantly different compared with the control

group (2/5) ($p < 0.05$). At 14 days, all ears were completely healed except one TM in the control group (4/5). By 28 days postsurgery, all the TMs had completely healed.

Scanning electron microscopy. The medial aspect of TMs was observed with SEM to assess scaffold attachment, cellular integration with scaffold, and perforation closure (Fig. 3A). The SFS and ACS showed steady attachment to the

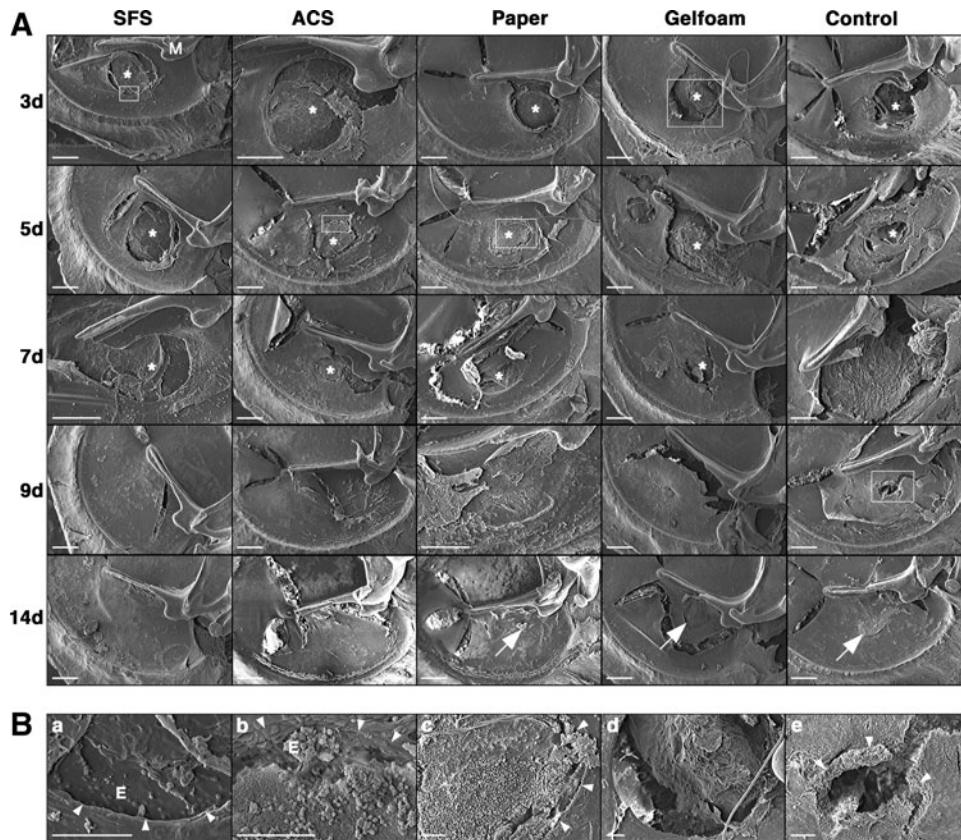


FIG. 3. Scanning electron microscopic observation of TM healing after grafting. The medial aspect of TMs was observed with SEM (A). SEM confirmed the attachment of SFS and ACS to the perforation margin throughout the healing process. TM epithelial cells were seen to have migrated to the medial surface of SFS on day 3 (B-a; $\times 500$) and ACS on day 5 (B-b; $\times 500$). TMs grafted with ACS and SFS had healed on day 9, where the medial surface of neo-membranes was smooth. Paper patch showed partial detachment from the TM surface on day 3. Exudate and inflammatory cell infiltration was evident at the perforation site on day 5 (B-c; $\times 150$). Gelfoam showed early disintegration with a majority of Gelfoam dissolving by day 3 (B-d; $\times 100$). At 14 days, the healed TMs in paper patch and Gelfoam groups showed some scarring (white arrows). In the control group, a rolled perforation edge in the unhealed TM was evident at 9 days (B-e; $\times 150$), and the TM healed by 14 days with an obvious scar (white arrow). Tears in the TMs were artefacts during the drying process. Asterisks indicate scaffolds; white arrowheads indicate perforation margin. M, handle of malleus; E, epithelial cells. Scale bar: 500 μm.

perforation margin throughout the healing process, thereby preserving their scaffold function. TM epithelial cells migrated across the wound margin and adhered to the internal surface of SFS on day 3 (Fig. 3B-a) and to ACS on day 5 (Fig. 3B-b). By 9 days, the TMs of both groups had healed, and the internal surface of neo-membranes was smooth. In contrast, paper patch demonstrated early partial detachment from the TM surface, and its scaffold function was partially lost. Exudate formation and inflammatory cell infiltration were evident at the perforation site in the paper group (Fig. 3B-c). Gelfoam showed early disintegration of its sponge structure (Fig. 3B-d). As shrinkage and absorption progressed, most of the Gelfoam dissolved, resulting in loss of its support function. The healed TMs in paper and Gelfoam groups showed some scarring at 14 days. In the control group with no scaffold implantation, a rolled perforation edge of the unhealed TM was visible at 9 days (Fig. 3B-e). The TM eventually healed by 14 days, but with an obvious scar.

Histological evaluation. The histology of the TM healing and effects of the four scaffolds were examined over 28 days (Fig. 4). Compared with other groups, TM healing in the control group was relatively slower. In the first week, the perforation remained patent, although hyperplasia was

observed in the epithelial and connective tissue (CT) layers of the TM. On day 5, a keratin spur was seen, and the perforations started closing at 9 days with significant thickening throughout the three TM layers. By 28 days, the healed TM became thinner but with residual thickening at the previous perforation site. The CT layer was found to be disorganized with loosely packed collagen fibers (Fig. 5I, L).

In the SFS group, TM healing was characterized by prominent hyperplasia of the epithelial and CT layers as well as at the perforation edge. The perforation was seen to close early at 7 days. By 28 days, the structure of healed TM appeared normal, with three obvious layers consisting of dense, well-organized collagen fibers in the middle layer (Fig. 5B, E). Throughout the healing process, only a minor inflammatory response was observed. In the ACS group, epithelial hyperplasia and vascular proliferation were evident in the early stages (day 7). Infiltrating cells resembling fibroblasts were abundant in the CT layer with occasional lymphocytes surrounding the graft. At 28 days, the healed TM appeared normal with a trilaminar structure (Fig. 5C, F).

In contrast, numerous inflammatory cells (predominantly lymphocytes) and prominent exudate were observed surrounding the paper patch. Although the TM perforation eventually healed, the TM remained thickened with disorganization of the newly synthesized fibers (Fig. 5G, J).

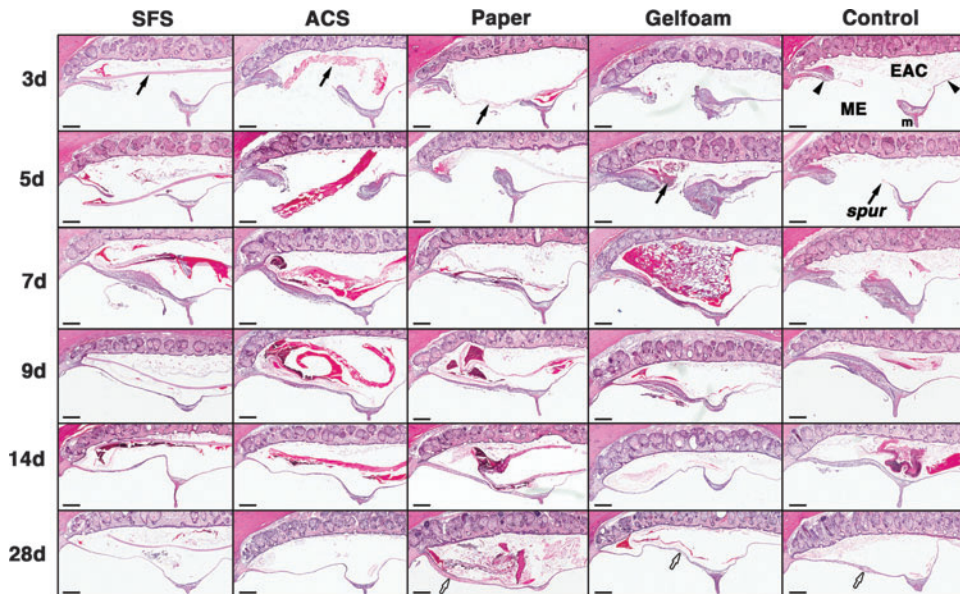


FIG. 4. Histological observation of the TM healing after grafting. In the SFS group, prominent hyperplasia was evident in the epithelial and connective tissue (CT) layers and at the perforation edge on days 3 and 5, with minor inflammatory responses seen throughout the healing process. In the ACS group, epithelial hyperplasia and vascular proliferation were evident in the early stages (day 3–7). Infiltrating cells resembling fibroblasts were abundant in the CT layer with a few lymphocytes surrounding the implant. The perforations in SFS and ACS groups closed early at 7 days, and the structure of healed TMs appeared normal at 28 days. Paper patch elicited lymphocytic cell infiltration with prominent exudates at 9–28 days. Gelfoam also induced the infiltration of inflammatory cells, and fibroblast proliferation was prominent in the CT layer. The perforations in paper and Gelfoam groups closed on days 7 and 9, respectively, with atypical and thickened healed TMs at 28 days (white arrows). In the control group, TM healing was relatively slower compared with scaffold-treated groups. The perforation remained patent in the first week, and a keratin spur was seen on day 5. The perforation had closed at 9 days with significant thickening throughout the three TM layers. By 28 days, the healed TM became thinner with residual thickening at the previous perforation site (white arrow). Black arrowheads indicate TMs; black arrows indicate scaffolds. EAC, external auditory canal; ME, middle ear; m, handle of malleus; spur, keratin spur. Haematoxylin and eosin (H&E) staining. Scale bars: 200 μ m.

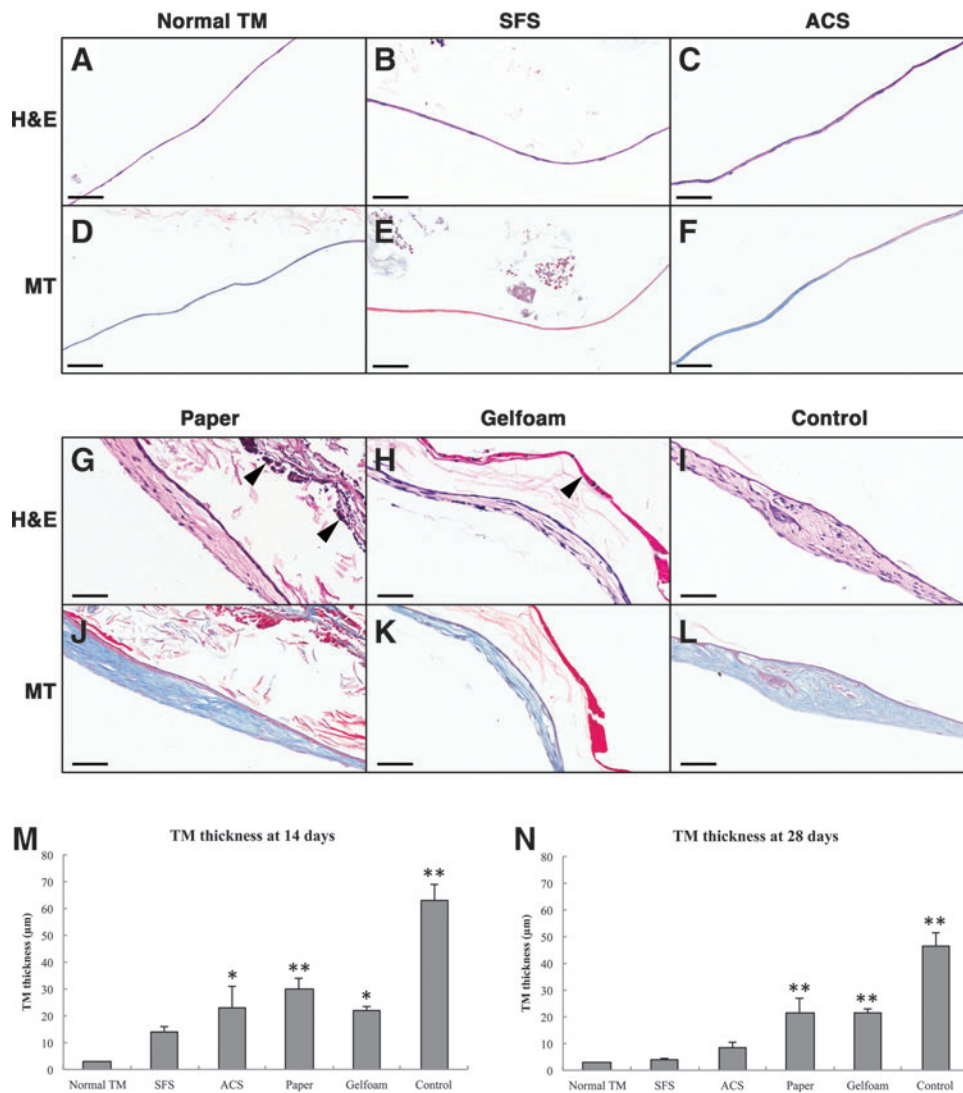


FIG. 5. Photomicrographs of healed TMs at 28 days after grafting. A normal TM shows a thin uniform structure (A, D). At 28 days, TMs treated with SFS (B, E) and ACS (C, F) had a normal trilaminar structure, consisting of dense and well-organized collagen bundles in the CT layer. TMs treated with paper patch (G, J) and Gelfoam (H, K) remained thickened in the healed area with loose and disorganized collagen fibers in the middle layer. TMs in the control group (I, L) remained thick with an atypical structure and regions of irregular collagen fibers. At 14 days, all TMs except the SFS group were significantly thickened compared with the normal TM (M). By 28 days, TM thickness in the SFS and ACS groups showed no significant differences compared with the normal TM (N). (* $p < 0.05$, ** $p < 0.01$). Arrowheads indicate the residual scaffolds. H&E and Masson trichrome staining. Scale bars: 50 µm.

Likewise, Gelfoam induced the infiltration of inflammatory cells at the implanted site. Unlike other materials, prominent fibroblast proliferation and erythrocyte-filled blood vessels were found in the CT layer. After 28 days, the healed TM remained thickened with atypical disorganized collagen fibers in the CT layer (Fig. 5H, K).

The TM cross-sections were used to quantify changes in the TM thickness after treatment (Fig. 5M, N). At 14 days, TMs in all groups were substantially thickened compared with normal TM ($p < 0.05$) except SFS-treated TM, which had a similar thickness ($14.13 \pm 4.04 \mu\text{m}$) to the normal TM ($p > 0.05$). By 28 days, statistically significant differences in TM thicknesses were found in the control, paper patch, and Gelfoam groups ($p < 0.05$). However, no statistically significant difference in TM thicknesses was seen in SFS ($4.01 \pm 0.63 \mu\text{m}$) and ACS groups ($8.55 \pm 4.25 \mu\text{m}$) compared with the normal TM ($p > 0.05$).

Ultrastructural morphology. TEM was performed to investigate the ultrastructure of healed TMs 28 days post-surgery. In scaffold-treated and spontaneously healed TMs, the CT layer was moderately thickened, and fibroblast

proliferation was apparent compared with the normal TM (Fig. 6B-F). In SFS and ACS groups, the three layers of the TM were readily identified, and the CT layer was compact with well-orientated collagen bundles (Fig. 6C, D). However, in paper patch and Gelfoam groups, collagen fibers were loosely and irregularly arranged in the fibrous layer, with obvious edema seen (Fig. 6E, F).

Improvement of hearing induced by scaffolds

Hearing thresholds were similar in all treatment groups measured preperforation ($p > 0.05$) and postperforation ($p > 0.05$). The average auditory threshold of the normal rat was 15.0 dB, and this significantly increased to 29.5 dB after perforation, indicating that TM perforation caused significant hearing loss ($p < 0.01$). Audiometric assessment using ABR demonstrated hearing recovery for all groups after treatment (Fig. 7). The hearing recovery was defined as the difference between the auditory threshold immediately after perforation (prerepair) and at specific time points after grafting (postrepair). Auditory threshold of all rats recovered over time, and significant differences were observed when

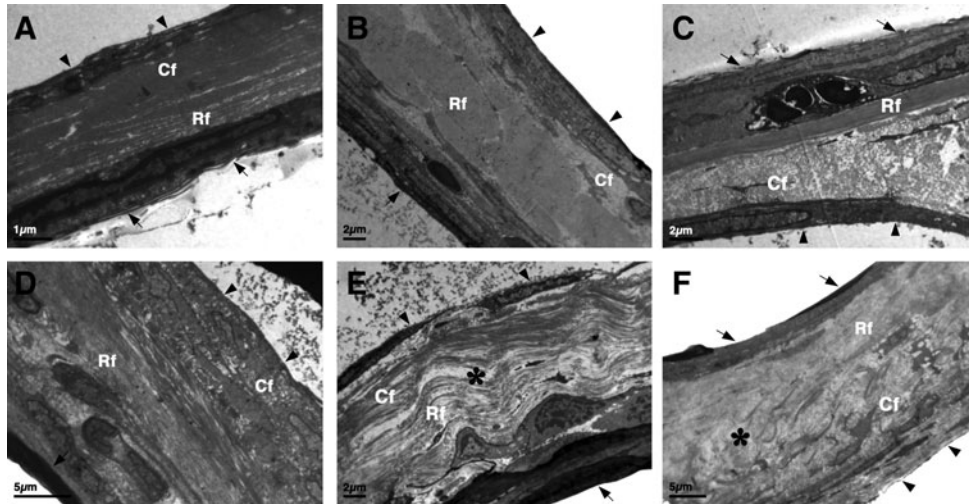


FIG. 6. Transmission electron microscopic observation of the TMs. Transmission electron microscopy images demonstrated the ultrastructure of a normal TM (A), spontaneously healed TM (B), and TMs repaired with SFS (C), ACS (D), paper patch (E), and Gelfoam (F) at 28 days. A normal TM (A) consists of an outer epidermal (arrows), middle CT, (containing radial fibers [Rf] and circular fibers [Cf]), and an inner mucosal layer (arrowheads). The CT layer was moderately thickened, and fibroblast proliferation was apparent in spontaneously healed (B) and scaffold-treated TMs (C–F). TMs repaired with SFS (C) and ACS (D) showed more compact tissues with dense, well-orientated collagen bundles compared with spontaneously healed TM (B) or TMs treated with paper patch (E) and Gelfoam (F). Edema (*) in the CT layer was apparent in paper patch (E) and Gelfoam (F) groups. Scale bars: A, 1 μm ; B, C, and E, 2 μm ; D and F, 5 μm .

comparing between different treatments ($p < 0.01$). Most obviously, hearing in the animals treated with the SFS or ACS recovered significantly faster compared with those treated with paper patch ($p < 0.05$ for SFS; $p < 0.01$ for ACS), Gelfoam ($p < 0.01$ for SFS and ACS), and spontaneous healing ($p < 0.01$ for SFS and ACS). Hearing recovery between SFS and ACS groups was similar ($p > 0.05$).

Discussion

This study demonstrated that two bioscaffolds (SFS and ACS) significantly shortened the perforation closure time

and promoted TM wound healing compared with two commonly used scaffolds (paper patch and Gelfoam) and spontaneous healing in a rat model. The healed TMs in SFS and ACS groups showed improved morphology with the regeneration of compact collagen fibers, a rapid return to a normal TM thickness, and complete hearing recovery at an earlier stage compared with the other groups. Since the goals of surgical treatment for TM perforation are to achieve complete closure of the perforation and restoration of the hearing,²⁷ these results suggest that both SFS and ACS are efficient and may serve as alternative scaffolds for improving both TM healing and hearing.

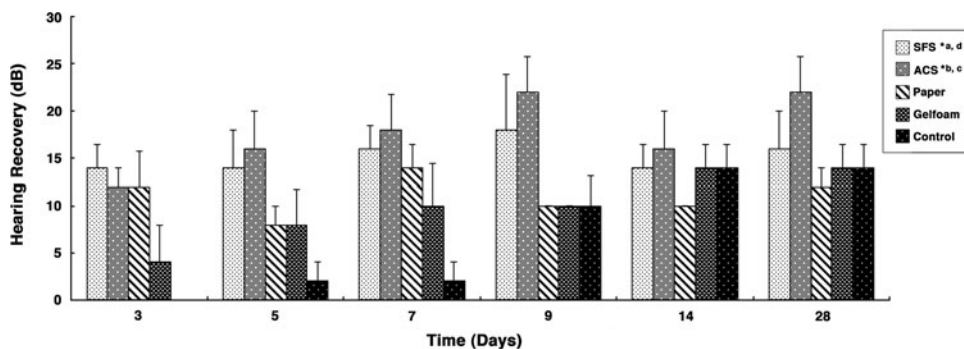


FIG. 7. Auditory brainstem responses assessment of hearing recovery after grafting. The hearing recovery was defined as the difference between auditory threshold immediately after perforation (prerepair) and at specific time points after grafting (postrepair). The values represent mean \pm standard error of mean ($n = 5$). Hearing recovery after grafting in each group was performed using multiple linear regression analysis. Auditory threshold of all rats recovered over time, and significant differences were observed when comparing between different treatments ($p < 0.01$). Hearing in the rats treated by the SFS or ACS recovered significantly faster compared with those treated with paper patch, Gelfoam, and spontaneous healing (control); however, no significant difference was found between SFS and ACS. Statistical significance between groups was as follows: ^aSFS and spontaneous healing ($p < 0.01$); SFS and Gelfoam ($p < 0.01$); ^bACS and spontaneous healing ($p < 0.01$); ACS and paper ($p < 0.01$); ACS and Gelfoam ($p < 0.01$); ^cSFS and ACS ($p > 0.05$); and ^dSFS and paper ($p < 0.05$).

In this study, it was evident that the use of scaffolds enhanced TM wound regeneration when compared with spontaneous healing. Scaffolds provided structural support in guiding the regenerating tissue across the perforation as seen with SEM. Moreover, scaffolds improved structural organization of the healed TMs and resulted in prominent hyperplasia of the epithelial and CT as observed via histology. Cell in-growth into the pores of scaffolds and integration of the scaffolds into healed TM were not observed, suggesting that scaffolds used with this on-lay technique serve to provide structural support rather than form a part of the regenerated TM. This finding is different in studies in which three-dimensional scaffolds are placed with an in-lay technique and found to integrate into the regenerated TM.²⁸ Among the four scaffolds used, SFS and ACS were found to attach closely to the TM perforation margin. In contrast, paper patch was found to attach weakly and was often lost from the TM surface whereas Gelfoam rapidly lost its sponge-like structure with evident swelling and shrinking. Paper and Gelfoam were unstable and detached early from the TM remnant, thereby losing their scaffold function and resulting in a delay in healing and resultant hearing. Where no scaffold was used in the spontaneously healed TMs, a keratin spur was observed on day 5. This keratin spur was thought to serve as a natural scaffold for the epithelium to bridge the perforation,²⁹ suggesting that scaffolds are indeed essential in promoting TM wound healing by providing support for early migration of keratinocytes. This is particularly important for TM repair, as the wound margin is suspended in air without an underlying tissue matrix that supports the regenerating epithelium and migrating neovasculature.³⁰

Our study showed that SFS achieved earlier structural repair of TM compared with paper patch and spontaneous healing. This is similar to a recently published study by Kim *et al.*¹³ They reported a significantly shorter healing time (1.9 days) between aqueous-based silk and paper patch; however, they did not report the hearing outcome. ACS also achieved similar outcomes as SFS in this study. Although previous studies have shown promising results for collagen membranes for TM reconstruction,^{14,31,32} no commonly used scaffolds were used as control materials in these studies, and different animal models were used. AlloDerm, a decellularized extracellular matrix in which the main component is collagen, has recently reported high perforation closure rates (87.5% to 100%).³³ However, its therapeutic capacity is restricted by its cadaveric origin, with a limited supply by tissue donations. Compared with AlloDerm, the porcine-derived ACS has been fashioned to a similar thickness to TM and, thus, provides a unique alternative for tympanic reconstruction. In terms of paper patch, our study showed similar results to previous research in terms of biocompatibility, fragility, and poor adhesion.^{8,16,34} Recent clinical trials showed encouraging results of Gelfoam patching for acute or small TM perforations.^{35,36} However, Gelfoam should be carefully applied, as it has been shown to cause adhesion, fibrosis, and even osteoneogenesis in the middle ear.³⁷⁻⁴⁰

In addition to a more rapid healing rate, our study also demonstrated that SFS and ACS achieved significantly faster hearing recovery compared with the other groups. A possible explanation may relate to improved organization of collagen fibers of healed TMs and early remodeling to achieve

comparable thickness to a normal TM. On the other hand, the healed TMs treated with paper patch, Gelfoam, and especially the spontaneous healing groups remained thickened with loosely disorganized collagen fibers accompanied by edema in the lamina propria layer. Since this lamina propria layer is critical in maintaining the mechanical and vibroacoustic properties of the TM, spontaneously healed TMs tend to result in higher reperforation rates and suboptimal hearing outcomes, particularly where a dimeric structure lacking the middle fibrous layer is formed. In addition, collagen fibers are essential in the preservation of the anatomical integrity of a TM by avoiding a retraction pocket caused by negative ME pressure.²⁴ In clinical practice, retraction pockets in weakened TMs result in complications such as cholesteatoma, which can be destructive and require further surgeries as well as adhesive fibrous otitis media, which can result in suboptimal hearing.^{41,42} Moreover, radial collagen fibers in the TM have been proved to be essential for sound conduction, especially in frequencies above 4 kHz.⁴³ In clinical cases with unsatisfactory hearing, it was found that the collagen fibers had not been restored, despite the reestablishment of an intact TM.⁴³

The requirements for an ideal TM scaffold include biocompatibility, biodegradability, and appropriate physical properties.¹⁶ More importantly, a bioscaffold should be safe and nonototoxic. All materials selected in this study have previously been found to be nonototoxic when packed into the middle ear cavity over 12 weeks in rats (Y. Shen, unpublished data). Recent studies have shown silk fibroin to be cytocompatible, free of toxicity and genotoxicity.⁴⁴ Collagen has also been known to be nonreactive, nontoxic, and noncarcinogenic^{7,22}; hence, many collagen-based materials have been approved by the Food and Drug Administration (FDA). Since the introduction of Gelfoam in 1945, it has been extensively used in otology mainly as a middle ear packing agent due to its nonantigenicity and nontoxicity.³⁷ Paper patch has also been used in outpatients for decades, as it is well tolerated with no severe complications reported to date.

Biocompatibility of a scaffold is an important element to be considered, as an inflammatory response after the application of biomaterials may lead to failure in surgery.^{11,45} In this study, the SFS and ACS accelerated and improved TM healing, partly attributed to minimal inflammatory response at the implantation sites, which is consistent with previous reports.^{13,32} The biocompatibility of SFS has been established after the removal of sericin, an antigenic glue-like coating protein.¹⁸ We recently showed its biocompatibility and ability to support human TM keratinocyte growth *in vitro*.^{20,21} Collagen is also known to elicit minimal inflammatory and antigenic responses⁴⁶; however, previous research showed unsatisfactory results with collagen films in repairing TM perforation due to unfavorable collagen purification.¹⁴ The ACS used in this study is acellular and contained no remaining reactive DNA that can invoke an inflammatory response. In contrast, we found that the paper patch was associated with severe inflammation, which may contribute to the delayed healing seen. With Gelfoam, only moderate inflammation was observed; however, complications such as adhesion and fibrosis may occur when it is used in the ME cavity.⁴⁰

Finally, physical properties of a scaffold should be considered. SFS and ACS were found to be easy to handle

during surgery, as they are not as fragile as paper or bulky and spongy as Gelfoam. Moreover, the transparency of SFS and ACS allowed direct observation of the TM, whereas the opacity of paper and Gelfoam obstruct the direct visibility of TM healing. From a clinical point of view, these characteristics make SFS and ACS more favorable compared with paper and Gelfoam. Although Gelfoam was significantly thicker compared with other materials, the thickness of the scaffold was not found to be a significant factor in the delay of TM wound healing.

With the advances in tissue engineering and biomaterials, recent research has focused on using tissue engineering techniques for TM reconstruction. With encouraging results, this regenerative method has been described as potentially the "greatest advance in otology since the cochlear implant."⁴⁷ Compared with conventional surgery, it is clear that tissue-engineered constructs could be applied in an outpatient setting without needing a surgery, with obvious cost and accessibility benefits. Although many biomaterials have been investigated, an ideal scaffold does not exist. Based on the findings of our studies, SFS and ACS are promising scaffolds for a bio-engineered TM. More importantly, improved TM healing with these materials may reduce complications such as recurrent otorrhea, middle ear infection, and acquired cholesteatoma.

A limitation of this study was the use of an acute rat TM perforation model, due to the lack of a robust and reliable animal model for chronic TM perforation.⁴⁸ TM perforations in rodents tend to heal naturally and rapidly⁴⁹ as was confirmed in this study; hence, further studies in a larger animal model (e.g., rabbit or monkey) may be needed. In addition, another limitation of the rat model is that the more commonly used scaffolds such as temporalis fascia were not used as controls due to the lack of this material in rats.⁵⁰ Despite these limitations of our model, we have identified a residual scarring and thickening within the time frame for our study and also demonstrated that the TM regeneration significantly improved when scaffolds were used, with less scarring and a rapid improvement to hearing. Hence, while these results may not extrapolate directly to chronic perforations in the clinical setting, they show encouraging improvements and indicate that further investigation in a suitable chronic perforation model may prove worthwhile.

Conclusion

In summary, this study showed that both SFS and ACS significantly accelerated acute TM wound healing and achieved hearing recovery from an early stage. The healed TMs in SFS and ACS groups demonstrated better morphology, comparable thickness to a normal TM, and improved organization of collagen fibers in the CT layer. Improved morphology was associated with significantly faster hearing recovery compared with the paper patch, Gelfoam, and spontaneous healing. In contrast, paper patch and Gelfoam lost their scaffold function in the early stages and showed an inflammatory response, which may have contributed to delayed healing. SFS and ACS also satisfy the requirements of an optimal scaffold for TM tissue engineering, including safety and biocompatibility, and have appropriate physical properties such as transparency and ease of handling, making them more favorable in the clinical setting. Taken

together, these data show that both SFS and ACS are comparatively better than Gelfoam, paper, and spontaneous healing and are potential clinical substitutes in the repair of TM perforations.

Acknowledgments

Yi Shen is supported by a Scholarship for International Research Fees (SIRF), University International Stipend (UIS), and UIS Safety-net Top-up Scholarship, The University of Western Australia. Yi Shen is also supported by Ningbo Lihuli Hospital (Ningbo Medical Centre) of the People's Republic of China as a Research Fellow at the University of Western Australia and the Ear Science Institute Australia. The authors express their gratitude to Dr. Rangam Rajkhowa from the Institute for Frontier Materials, Deakin University, Geelong, for manufacturing and providing the silk fibroin membranes used in this study. They acknowledge the facilities, scientific and technical assistance rendered by the Australian Microscopy and Microanalysis Research Facility at the Center for Microscopy, Characterization, and Analysis, The University of Western Australia, a facility funded by the University, State, and Commonwealth Governments. This work is partly supported by the grant from 863 Scaffold Project of China (No. 2012AA020501) to Minghao Zheng, and a linkage grant from the Australia Research Council (No. 110200547).

Disclosure Statement

Minghao Zheng is the inventor of the collagen scaffold patent and receives consultancy from Orthocell Ltd., Australia.

References

1. Parekh, A., Mantle, B., Banks, J., Swarts, J.D., Badylak, S.F., Dohar, J.E., and Hebda, P.A. Repair of the tympanic membrane with urinary bladder matrix. *Laryngoscope* **119**, 1206, 2009.
2. Lindeman, P., Edstrom, S., Granstrom, G., Jacobsson, S., von Sydow, C., Westin, T., and Aberg, B. Acute traumatic tympanic membrane perforations: cover or observe? *Arch Otolaryngol Head Neck Surg* **113**, 1285, 1987.
3. Sheehy, J.L., and Anderson, R.G. Myringoplasty. A review of 472 cases. *Ann Otol Rhinol Laryngol* **89**, 331, 1980.
4. Karela, M., Berry, S., Watkins, A., and Phillipps, J.J. Myringoplasty: surgical outcomes and hearing improvement: is it worth performing to improve hearing? *Eur Arch Otorhinolaryngol* **265**, 1039, 2008.
5. Levin, B., Rajkhowa, R., Redmond, S.L., and Atlas, M.D. Grafts in myringoplasty: utilizing a silk fibroin scaffold as a novel device. *Expert Rev Med Devices* **6**, 653, 2009.
6. Spiegel, J.H., and Kessler, J.L. Tympanic membrane perforation repair with acellular porcine submucosa. *Otol Neurotol* **26**, 563, 2005.
7. Abbenhaus, J.I. The use of reconstituted bovine collagen for tympanic membrane grafting. *Otolaryngology* **86**, 485, 1978.
8. Golz, A., Goldenberg, D., Netzer, A., Fradis, M., Westerman, S.T., Westerman, L.M., and Joachims, H.Z. Paper patching for chronic tympanic membrane perforations. *Otolaryngol Head Neck Surg* **128**, 565, 2003.
9. Teh, B.M., Shen, Y., Friedland, P.L., Atlas, M.D., and Marano, R.J. A review on the use of hyaluronic acid in

- tympenic membrane wound healing. *Expert Opin Biol Ther* **12**, 23, 2012.
10. Aggarwal, R., Saeed, S.R., and Green, K.J. Myringoplasty. *J Laryngol Otol* **120**, 429, 2006.
 11. Zheng, M.H., Chen, J., Kirilak, Y., Willers, C., Xu, J., and Wood, D. Porcine small intestine submucosa (SIS) is not an acellular collagenous matrix and contains porcine DNA: possible implications in human implantation. *J Biomed Mater Res B Appl Biomater* **73**, 61, 2005.
 12. Gilbert, T.W., Freund, J.M., and Badylak, S.F. Quantification of DNA in biologic scaffold materials. *J Surg Res* **152**, 135, 2009.
 13. Kim, J., Kim, C.H., Park, C.H., Seo, J.N., Kweon, H., Kang, S.W., and Lee, K.G. Comparison of methods for the repair of acute tympanic membrane perforations: Silk patch vs. paper patch. *Wound Repair Regen* **18**, 132, 2010.
 14. Bonzon, N., Carrat, X., Deminière, C., Daculsi, G., Lefebvre, F., and Rabaud, M. New artificial connective matrix made of fibrin monomers, elastin peptides and type I+III collagens: structural study, biocompatibility and use as tympanic membranes in rabbit. *Biomaterials* **16**, 881, 1995.
 15. Hakuba, N., Iwanaga, M., Tanaka, S., Hiratsuka, Y., Kumabe, Y., Konishi, M., Okanou, Y., Hiwatashi, N., and Wada, T. Basic fibroblast growth factor combined with atelocollagen for closing chronic tympanic membrane perforations in 87 patients. *Otol Neurotol* **31**, 118, 2010.
 16. Kim, J.H., Choi, S.J., Park, J.S., Lim, K.T., Choung, P.H., Kim, S.W., Lee, J.B., Chung, J.H., and Choung, Y.H. Tympanic membrane regeneration using a water-soluble chitosan patch. *Tissue Eng Part A* **16**, 225, 2009.
 17. Hott, M.E., Megerian, C.A., Beane, R., and Bonassar, L.J. Fabrication of tissue engineered tympanic membrane patches using computer-aided design and injection molding. *Laryngoscope* **114**, 1290, 2004.
 18. Altman, G.H., Diaz, F., Jakuba, C., Calabro, T., Horan, R.L., Chen, J., Lu, H., Richmond, J., and Kaplan, D.L. Silk-based biomaterials. *Biomaterials* **24**, 401, 2003.
 19. Weber, D.E., Semaan, M.T., Wasman, J.K., Beane, R., Bonassar, L.J., and Megerian, C.A. Tissue-Engineered calcium alginate patches in the repair of chronic chinchilla tympanic membrane perforations. *Laryngoscope* **116**, 700, 2006.
 20. Levin, B., Redmond, S.L., Rajkhowa, R., Eikelboom, R.H., Marano, R.J., and Atlas, M.D. Preliminary results of the application of a silk fibroin scaffold to otology. *Otolaryngol Head Neck Surg* **142**, S33, 2010.
 21. Ghassemifar, R., Redmond, S., Zainuddin, and Chirila, T.V. Advancing towards a tissue-engineered tympanic membrane: silk fibroin as a substratum for growing human eardrum keratinocytes. *J Biomater Appl* **24**, 591, 2010.
 22. Patterson, M.E. Experimental tympanic membrane closure with collagen film. *Arch Otolaryngol* **86**, 486, 1967.
 23. Knutsson, J., Bagger-Sjöbäck, D., and von Unge, M. Distribution of different collagen types in the rat's tympanic membrane and its suspending structures. *Otol Neurotol* **28**, 486, 2007.
 24. Knutsson, J., Bagger-Sjöbäck, D., and von Unge, M. Collagen type distribution in the healthy human tympanic membrane. *Otol Neurotol* **30**, 1225, 2009.
 25. Rajkhowa, R., Levin, B., Redmond, S.L., Li, L.H., Wang, L., Kanwar, J.R., Atlas, M.D., and Wang, X. Structure and properties of biomedical films prepared from aqueous and acidic silk fibroin solutions. *J Biomed Mater Res A* **97A**, 37, 2011.
 26. Rohanzadeh, R., Swain, M.V., and Mason, R.S. Gelatin sponges (Gelfoam) as a scaffold for osteoblasts. *J Mater Sci Mater Med* **19**, 1173, 2008.
 27. Albera, R., Ferrero, V., Lacilla, M., and Canale, A. Tympanic reperforation in myringoplasty: evaluation of prognostic factors. *Ann Otol Rhinol Laryngol* **115**, 875, 2006.
 28. Kim, J., Kim, S.W., Choi, S.J., Lim, K.T., Lee, J.B., Seonwoo, H., Choung, P.H., Park, K., Cho, C.S., Choung, Y.H., and Chung, J.H. A healing method of tympanic membrane perforations using three-dimensional porous chitosan scaffolds. *Tissue Eng Part A* **17**, 2763, 2011.
 29. Spandow, O., Hellström, S., and Dahlström, M. Structural characterization of persistent tympanic membrane perforations in man. *Laryngoscope* **106**, 346, 1996.
 30. Santa Maria, P.L., Redmond, S.L., Atlas, M.D., and Ghassemifar, R. Histology of the healing tympanic membrane following perforation in rats. *Laryngoscope* **120**, 2061, 2010.
 31. Morgon, A., Disant, F., and Truy, E. Experimental study of collagen as eardrum graft support in dogs. *Acta Otolaryngol* **107**, 450, 1989.
 32. Truy, E., Disant, F., Tiollier, J., Froehlich, P., and Morgon, A. A clinical study of human type IV collagen as tympanic membrane grafting material. Preliminary noncomparative study. *Arch Otolaryngol Head Neck Surg* **120**, 1329, 1994.
 33. Haynes, D.S., Vos, J.D., and Labadie, R.F. Acellular allograft dermal matrix for tympanoplasty. *Curr Opin Otolaryngol Head Neck Surg* **13**, 283, 2005.
 34. Chun, S.H., Lee, D.W., and Shin, J.K. A clinical study of traumatic tympanic membrane perforation. *Korean J Otolaryngol* **23**, 437, 1999.
 35. Lou, Z.C., and He, J.G. A randomised controlled trial comparing spontaneous healing, gelfoam patching and edge-approximation plus gelfoam patching in traumatic tympanic membrane perforation with inverted or everted edges. *Clin Otolaryngol* **36**, 221, 2011.
 36. Niklasson, A., and Tano, K. The Gelfoam® plug: an alternative treatment for small eardrum perforations. *Laryngoscope* **121**, 782, 2011.
 37. Hellström, S., Salén, B., and Stenfors, L.E. Absorbable gelatin sponge (Gelfoam) in otosurgery: one cause of undesirable postoperative results? *Acta Otolaryngol* **96**, 269, 1983.
 38. Doyle-Kelly, W. Behaviour of absorbable gelatine sponge in the animal middle ear. *J Laryngol Otol* **75**, 152, 1961.
 39. Bahadir, O., Aydin, S., and Caylan, R. The effect on the middle-ear cavity of an absorbable gelatine sponge alone and with corticosteroids. *Eur Arch Otorhinolaryngol* **260**, 19, 2003.
 40. Shen, Y., Teh, B.M., Friedland, P.L., Eikelboom, R.H., and Atlas, M.D. To pack or not to pack? A contemporary review of middle ear packing agents. *Laryngoscope* **121**, 1040, 2011.
 41. Forsen, J.W. Chronic disorders of the middle ear and mastoid. In: Wetmore, R.F., Muntz, H.R., and McGill, T.J., eds. *Pediatric Otolaryngology, Principles and Practice Pathways*. NY: Thieme, 2000, pp. 281–304.
 42. Cassano, M., and Cassano, P. Retraction pockets of pars tensa in pediatric patients: clinical evolution and treatment. *Int J Pediatr Otorhinolaryngol* **74**, 178, 2010.
 43. O'Connor, K.N., Tam, M., Blevins, N.H., and Puria, S. Tympanic membrane collagen fibers: a key to high-frequency sound conduction. *Laryngoscope* **118**, 483, 2008.
 44. Liu, T.L., Miao, J.C., Sheng, W.H., Xie, Y.F., Huang, Q., Shan, Y.B., and Yang, J.C. Cytocompatibility of regenerated silk fibroin film: a medical biomaterial applicable to wound healing. *J Zhejiang Univ Sci B* **11**, 10, 2010.

45. Malcarney, H.L., Bonar, F., and Murrell, G.A. Early inflammatory reaction after rotator cuff repair with a porcine small intestine submucosal implant: a report of 4 cases. *Am J Sports Med* **33**, 907, 2005.
46. Pachence, J.M. Collagen-based devices for soft tissue repair. *J Biomed Mater Res* **33**, 35, 1996.
47. Jackler, R.K. A regenerative method of tympanic membrane repair could be the greatest advance in otology since the cochlear implant. *Otol Neurotol* **33**, 289, 2012.
48. Santa Maria, P.L., Atlas, M.D., and Ghassemifar, R. Chronic tympanic membrane perforation: a better animal model is needed. *Wound Repair Regen* **15**, 450, 2007.
49. Krupala, J.L., Gianoli, G.J., and Smith, R.A. The efficacy of hyaluronic acid foam as a middle ear packing agent in experimental tympanoplasty. *Am Otol* **19**, 546, 1998.
50. Schiller, A., and Wormald, P.J. Malleomyringoplasty using a silicone prosthesis. *J Laryngol Otol* **106**, 205, 1992.

Address correspondence to:

Robert Jeffery Marano, PhD

Ear Sciences Centre

School of Surgery (M507)

The University of Western Australia

Nedlands, WA 6009

Australia

E-mail: rob.marano@earsience.org.au

Minghao Zheng, PhD, MD, FRCPATH

Centre for Orthopaedics Research

School of Surgery (M508)

The University of Western Australia

Nedlands, WA 6009

Australia

E-mail: minghao.zheng@uwa.edu.au

Received: January 29, 2012

Accepted: September 25, 2012

Online Publication Date: December 10, 2012